Lawrence Berkeley National Laboratory
Recent Work

Title

SUPERSATURATION AT GAS-EVOLVING ELECTRODES

Permalink

https://escholarship.org/uc/item/5sd1p4tt

Author

Bon, Charles K.

Publication Date

1970-11-01

UCRL-19612

C.2

SUPERSATURATION AT GAS-EVOLVING ELECTRODES

Charles K. Bon
(M.S. Thesis)

September 1970

LAWRENCE RADIATION LABORATORY
UNIVERSITY of CALIFORNIA BERKELEY

UCRL-19612
c.2

DISCLAIMER

TABLE OF CONTENTS

SUPERSATURATION AT GAS-EVOLVING ELECTRODES

Charles K. Bon

Inorganic Materials Research Division
Lawrence Radiation Laboratory, and
Department of Chemical Engineering
University of California, Berkeley

September 1970

ABSTRACT

Equilibrium hydrogen electrodes were used to measure gas supersaturation near a horizontal cathode evolving hydrogen. The observed concentration gradients at the surface support the hypothesis that dissolved gas diffuses into the solution and thence to gas bubbles formed on the surface. The surface supersaturation at steady state is found to be proportional to the square root of the current density, increasing from 4 to 60 atmospheres in the range from 0.2 to 40 ma/cm^2. This result is in harmony with a surface-renewal model of the gas evolution process.

INTRODUCTION

In industrial processes as well as in laboratory investigations electrodes are frequently employed where one of the products is a gas. A complete study of any electrode reaction must involve consideration not only of the charge transfer steps, but also the transport of reactants and products to and from the electrodes. In the case of gas-generating electrodes mass transfer is complex, involving both convection and diffusion. Relatively few observations are available on the transport of gaseous products from an electrode. This report presents measurements of hydrogen supersaturation near a horizontal electrode with steady-state evolution of hydrogen from one and two molar sulfuric acid solutions.

When current is first applied to a gas generating electrode, before bubbles start to form, the gas diffuses into the bulk of the electrolyte and builds up a uniform concentration profile as shown in Fig. 1.

The gas concentration before bubble formation is obtained by integrating the diffusion equation[1] with boundary conditions of constant initial electrolyte concentration, and constant gas production rate (corresponding to constant current density). Equation (1) gives the gas concentration as a function of time and distance from the electrode.

$$C = C_B + \frac{2I}{nF}\sqrt{\frac{t}{D}} \text{ ierfc } \frac{x}{2\sqrt{Dt}} \tag{1}$$

In the absence of convection or bubble formation, Eq. (1) shows that the concentration at the electrode surface is proportional to the square root of time and continues to increase indefinitely (since ierfc

Electrode
before formation of bubbles
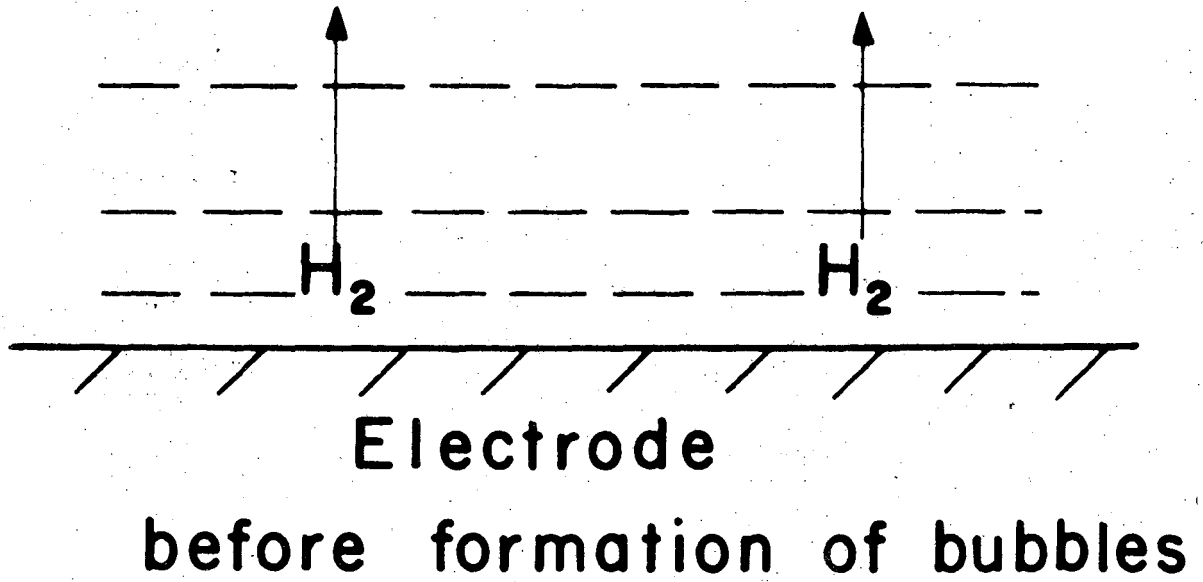
XBL 704-882

Fig. 1. Concentration profile of dissolved hydrogen gas at cathode before bubble formation.

(O) is constant with a value of 0.564). Figure 2 snows the concentration of dissolved hydrogen at a cathode surface as a function of time as calculated by using Eq. (1). The concentration versus distance from the cathode surface is shown in Fig. 3. Even at extremely low current densities some mechanism in addition to diffusion must contribute to remove gas at the rate it is being produced.

Removal of all the gas from an electrode without bubble formation is possible by supplying agitation to form an extremely thin boundary layer. If the boundary layer is thin enough, all the dissolved gas can diffuse to the bulk electrolyte where it can either form bubbles or escape from the electrolyte surface by convection. One of the most effective means of stirring is the rotating disc electrode. Using the solution of the convective diffusion equation for the rotating disc obtained by Levich,[2] we find for example, that at the surface of a disc rotating at 10,000 RPM, a current density of 20 mA/cm^2 should cause a steady state concentration of dissolved hydrogen gas corresponding to 2 atm* partial pressure.**

In the absence of vigorous external agitation, or at high current densities soon after the start of passage of current the concentration at the electrode becomes high enough to nucleate bubbles. At this point concentration profile changes to the type shown qualitatively in Fig. 4.

---

* Definition of symbols given in separate list.

** Solubility of H_2 at 1 atm 7.2 X 10^7 moles/cm^3 [3]

Diffusivity of H_2 3.8 X 10^5 cm^2/sec [4]
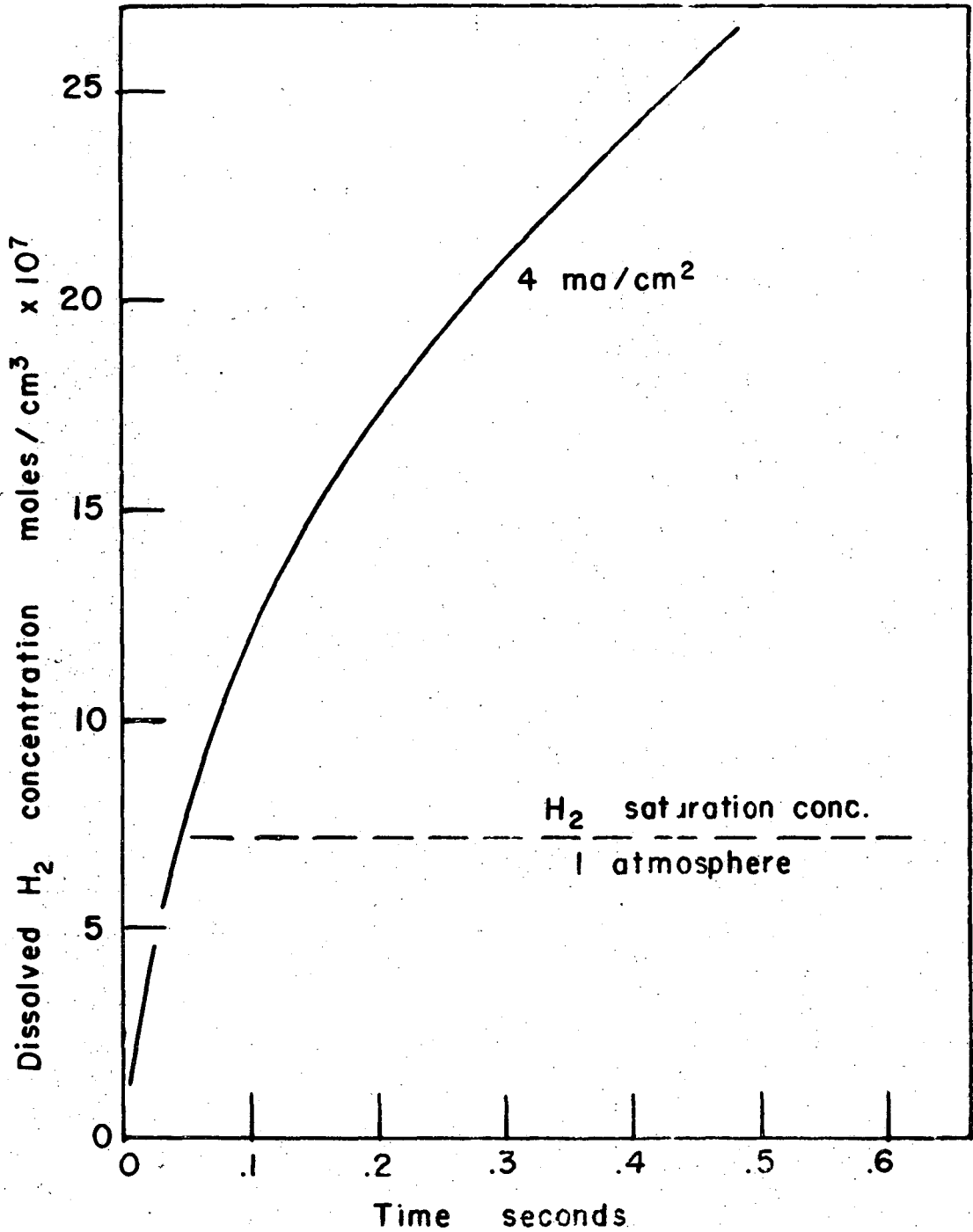
Fig. 2. Calculated concentration of dissolved hydrogen at cathode surface before bubble formation (stagnant electrolyte, D_{H_2} = 3.8 x $10^5 cm^2$/sec).

XBL 704-886

Fig. 3. Calculated concentration of dissolved hydrogen as a function of distance from cathode before bubble formation.

Gas now diffuses to bubbles at nearby locations on the cathode as well as to the bulk electrolyte. After the bubbles have grown to a critical size, determined by the surface tension, contact angle, and pressure forces,[5] they disengage from the surface. Eventually a steady process is established by diffusion near the cathode and by rising bubbles far from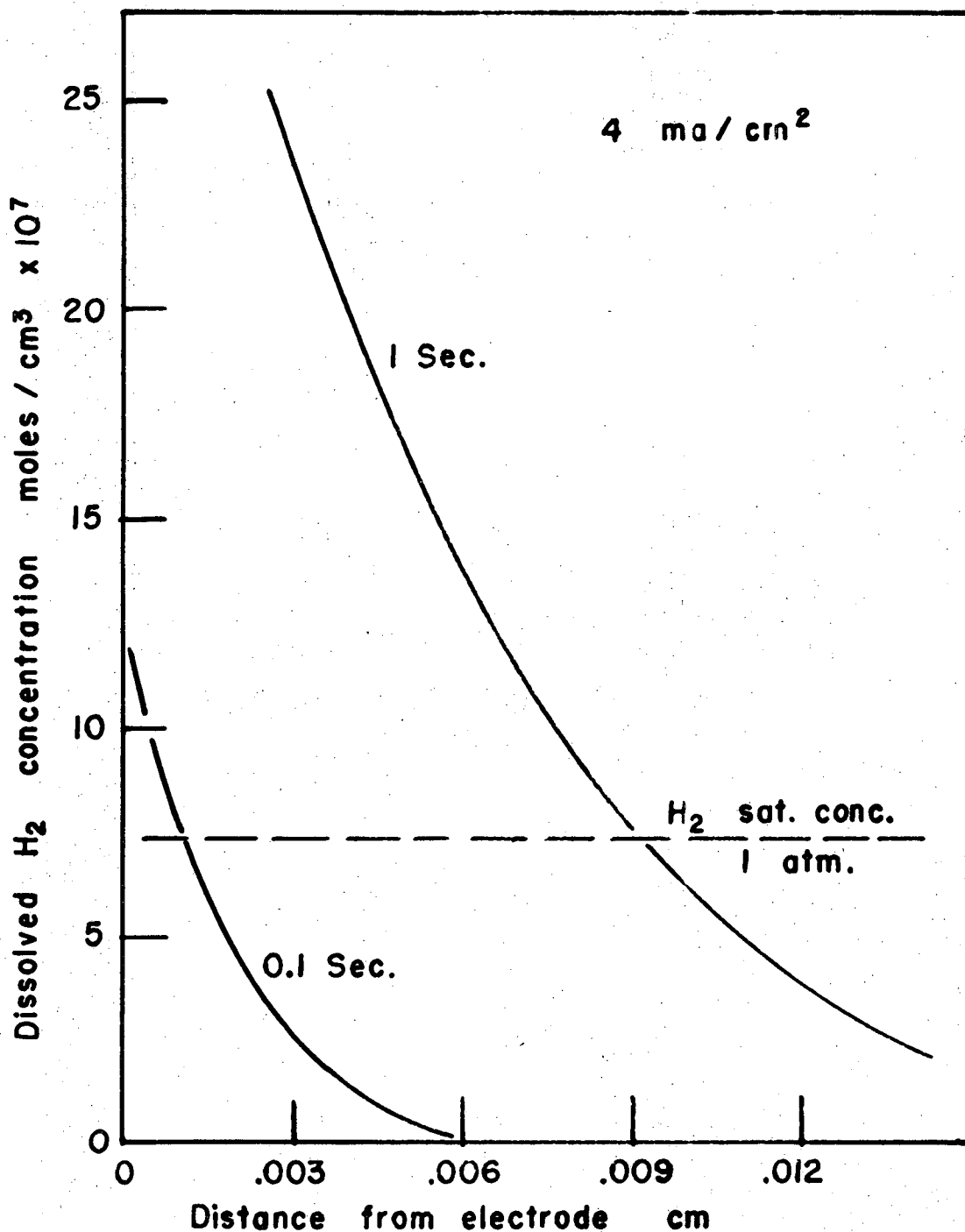 the cathode in which the vertical flux of hydrogen is uniform. The bubble motion causes effective stirring of the electrolyte and provides for convection as an additional mechanism of mass transfer. Convection is most significant at intermediate distances from the cathode; far enough so turbulence is important, but not so far that all excess hydrogen has been transferred to the gas phase.

The process of bubble evolution occurs in discrete steps causing the dissolved gas concentration at any point near the cathode to increase and decrease in a cyclic manner depending on the stage of growth of the bubbles in the immediate vicinity. For this reason there is no single exact value for the gas concentration at a given distance from the cathode even though the total hydrogen flux is a constant. Measured values of the supersaturation represent average concentrations.

Only within the last fifteen years have gas concentrations at electrode surfaces been reported. An AC phase-shifting technique was used by Breiter[6,7,8] and his co-workers to measure the hydrogen concentration at cathodes with low activation overvoltages. Lewis and Green[9] measured the hydrogen dissolved in the metal of a palladium cathode and calculated the hydrogen concentration in solution by assuming that the metal and the electrolyte were in equilibrium at the electrode surface. Glas and Westwater[10] have adopted an approach directed toward studying
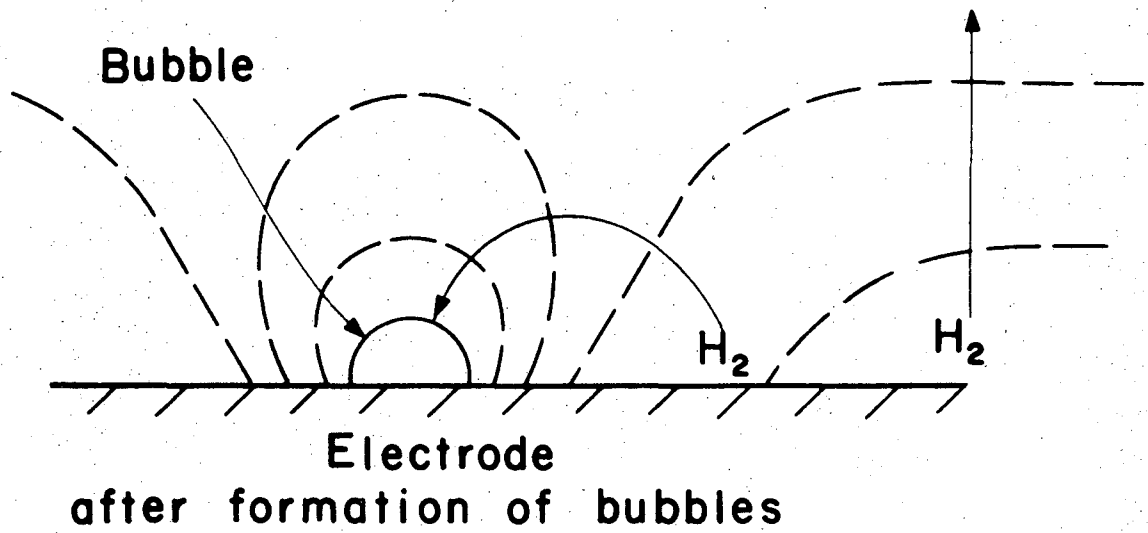
Fig. 4. Dissolved hydrogen concentration profile at cathode after formation of bubbles.

the mechanism of gas transport at an electrode by measuring the growth
rate of a single bubble. Cheh[11] has reviewed the entire mass transfer
process including nucleation, bubble growth, and disengagement. There
is, however, still no satisfactory method of predicting gas concentration
at an electrode. In this work the concentration of dissolved hydrogen
in the vicinity of a cathode is measured using platinized platinum
electrodes, and a simplified model is tested to correlate gas concentra-
tion at the electrode surface with current density.

EXPERIMENTAL

Cell Design

The principal tool for measuring hydrogen concentrations in the vicinity of the cathode was a cell equipped with hydrogen reference electrodes located within the cathode boundary layer. Figure 5 shows the schematic design of the cell. A laminated construction is used to locate the measuring electrodes at known distances from the cathode (inset Fig. 5). The measuring electrodes are sheets of 0.00062 cm platinum foil with sheets of plastic of various thicknesses separating them and determining the distance of each electrode above the cathode. Locations of the electrodes are given in Table I.

Table I

Electrode Number	Distance from cathode cm
1	0.0016
2	0.0035
3	0.0086
4	0.0137
5	0.0390
6	0.065
7	0.225
8	0.545

The layers of platinum and plastic are bolted to the bottom of a 7.5-cm diameter by 5-cm long cylinder of plastic which serves as the cell body, and a 1.25 cm hole is bored through the assembly and the
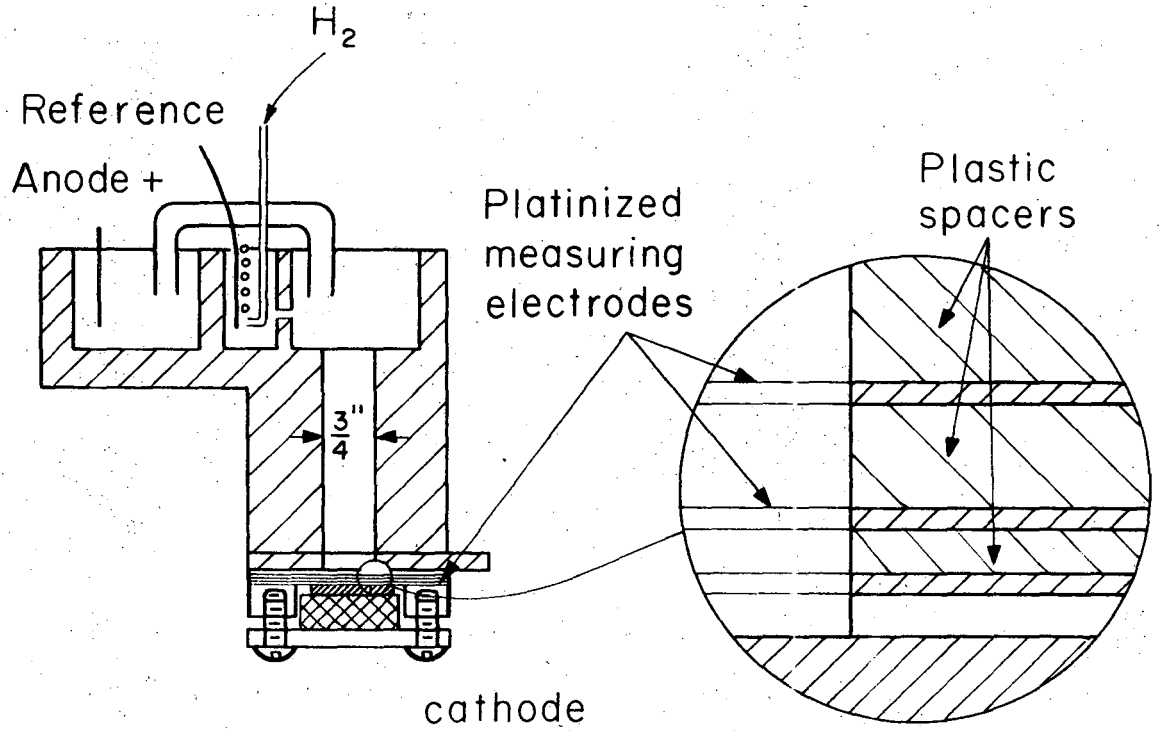
Fig. 5. Diagram of cell used for measuring dissolved hydrogen concentration in the vicinity of cathode.

plastic block. Polishing and platinizing the exposed edges of the platinum foil made the edge of each sheet a reversible hydrogen electrode flush with the cell wall. The electrolyte compartment is formed by bolting the cathode onto the bottom of the assembly. The straight walls of the cathode compartment parallel to the direction of current flow provide a geometry that gives a uniform cathode current density. The current distribution is not affected by the measuring electrodes.

The procedure for platinizing the measuring electrode was adapted from Ives and Janz.[12] The electrodes were cleaned by making them alternately anodes and cathodes in 1 $\underline{M}$ H_2SO_4 at a current density of 250 ma per cm^2. The platinum was deposited from a 3% platinic chloride solution containing .02% lead acetate. A current density of 15 ma/cm^2 was maintained for 10 minutes.

The geometry of the cell, where each measuring electrode has a length equal to the circumference of the cathode compartment provides the maximum active electrode area. Even though this active area ($2.4 \times 10^{-3} cm^2$) is below that recommended by Ives and Janz, the potentials were reproduceable to within ± 2 millivolts of the standard hydrogen electrode potential. Earlier attempts to use smaller electrode areas such as the platinized tip of a wire were unsuccessful because a bubble would cover an entire electrode area and cause erroneous readings. The platinum wires also caused abnormal current distribution in the vicinity of the measuring electrode when they were close enough to the cathode to be within the boundary layer.

The anode compartment was connected to the cathode compartment through an electrolyte bridge. This precaution insured that none of

the oxygen produced at the anode could reach the ring reference electrodes. Similarly, to prevent any influence of the oxygen from the anode the hydrogen electrode (1 atm), relative to which the potentials of the ring reference electrodes were measured, was also located in a separate chamber. The assembled cell ready for operation is shown in Fig. 6.

Cell Operation

Measurements were made with two different types of cathodes - one smooth platinum, and the other platinized. Both platinum cathodes were polished to a mirror finish mechanically, the final polish was obtained using one micron diamond dust. The platinized electrode was then cleaned in nitric acid. The coating was deposited from a 3% platinic chloride solution containing .02% lead acetate at a current density of 150 ma/cm^2 for 2 minutes.

Voltages were measured with an integrating digital voltmeter.* The meter records thirty voltages per second and could be programmed to record in sequence voltages from several different locations. Voltages measured in this manner also were checked with an electrometer.** Maximum discrepancy between the two instruments was less than one millivolt, which was within the reproduceability of the hydrogen measuring electrodes.

From the potential of the ring reference electrodes measured against the hydrogen electrode at 1 atm in the bulk electrolyte, the hydrogen gas concentrations were calculated using the Nernst equation. The gas

---

*Vidar system. "Vidar digital data acquisition system," consisting of vidar 520 integrating digital voltmeter, vidar 625 digital clock, vidar 12361-1 scanner (30 channels), vidar 650-8 coupler, Franklin High Speed Printer 1030D.

**Keithley system. 149 millimicrovoltmeter, or 601 electrometer, or 610R electrometer.
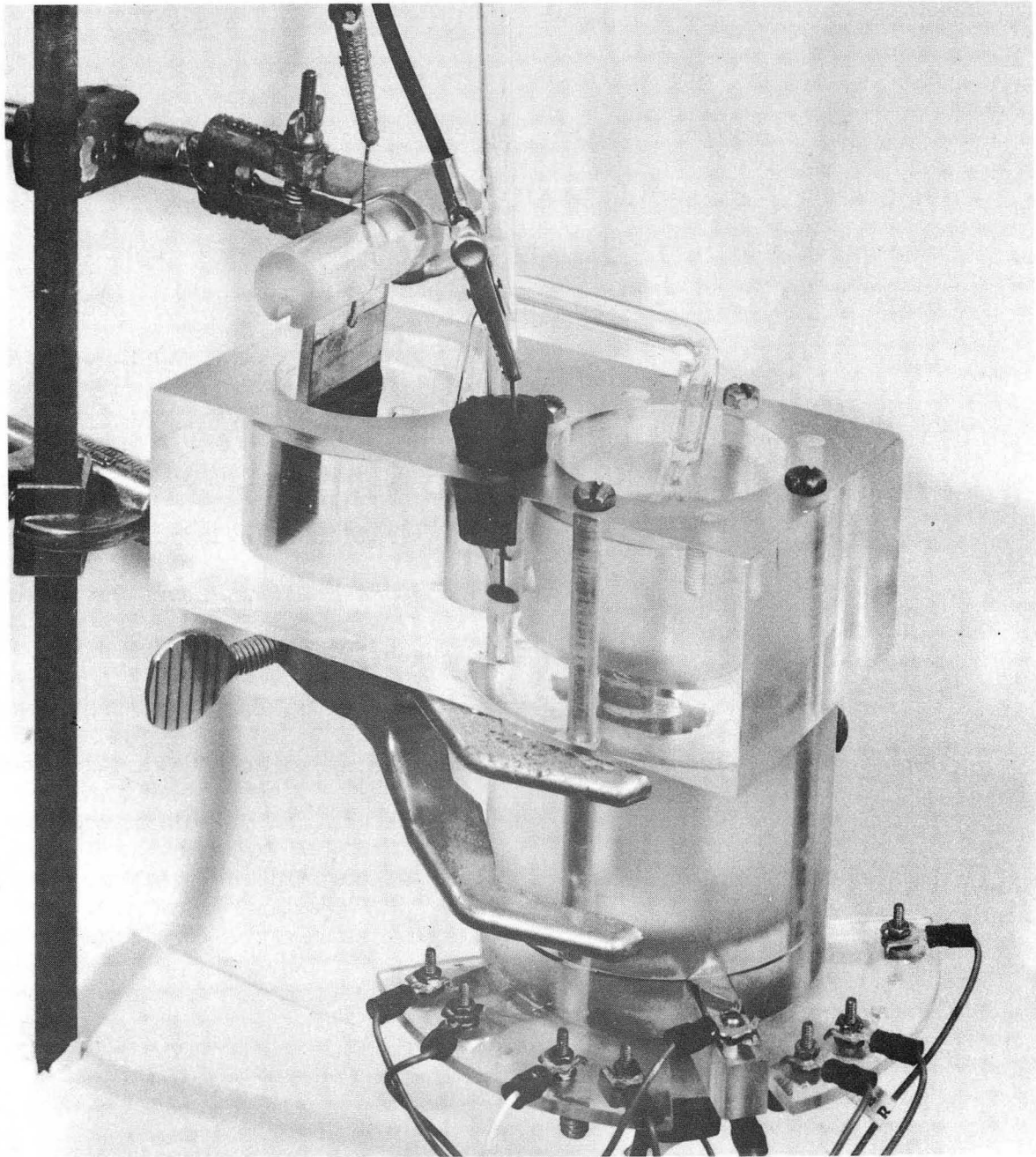
XBB677-4104

Fig. 6.   Photograph of the complete cell assembly.

concentration in the bulk electrolyte was maintained at one atmosphere by bubbling hydrogen into the top compartment of the cell and the reference electrode chamber. Hydrogen-ion concentration differences near the cathode were assumed to be negligible. Using Venezel's[13] measurements of mass-transport rates at gas-evolving electrodes as a basis for estimating the maximum shift of pH at the electrode, we find that at 40 mA/cm^2, the maximum current density employed in the present study, $\delta \simeq$ 0.003 cm. Thus the shift of potential caused by change of pH would be at the most 0.6 millivolts* $\sim$ less than 1% of the observed voltage difference caused by supersaturation of hydrogen.

After the current was turned on, the cell was operated until steady-state voltages were established. The slowest approach to steady state, approximately ten minutes, was observed at the lowest current density employed. A period of three minutes during which the voltage readings on all the electrodes remained constant was the criterion used to indicate the establishment of steady state. The current was then shut off to eliminate IR drop, and voltage measurements were made between the 1 atm reference electrode and each of the ring electrodes at intervals of 30 milliseconds.
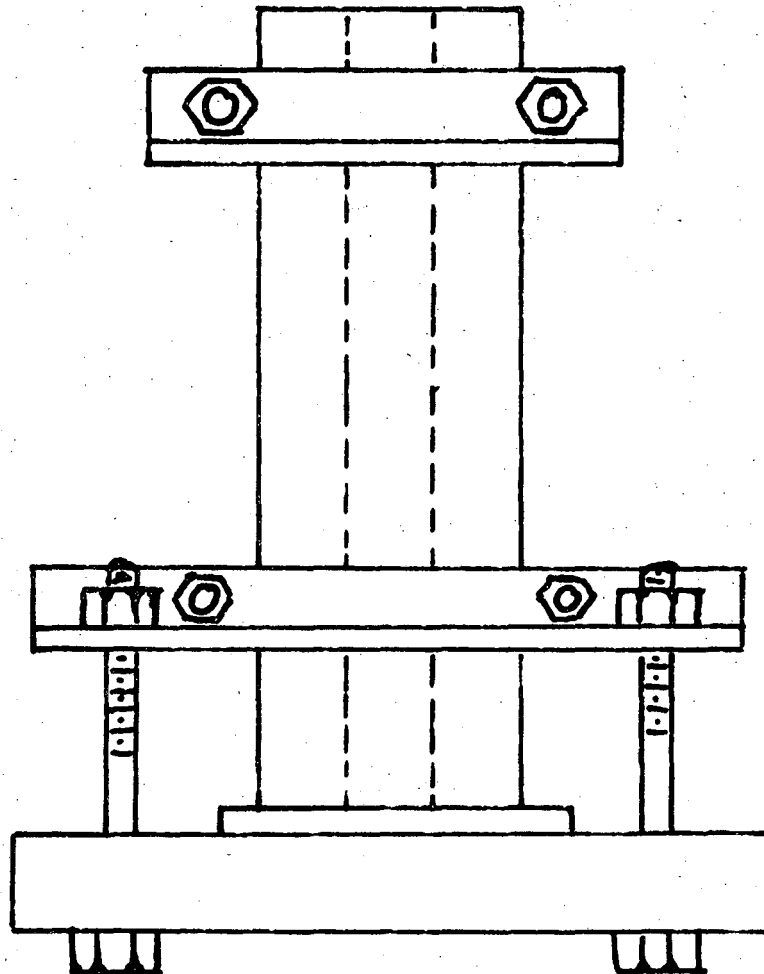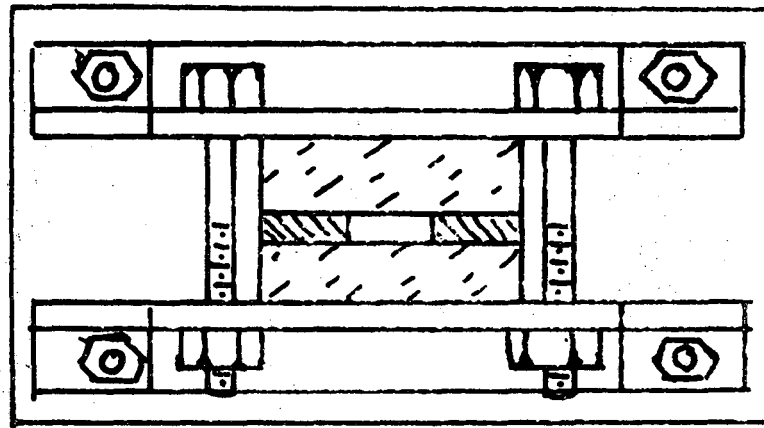
Bubble Size

In order to test a surface-renewal model for correlating hydrogen supersaturation with current density, data on the size of bubbles being discharged from the cathode are required. A special cell, shown in

---

*t_{H^+} = 0.808 in 1 $\underline{M}$ H_2SO_4[14]

$D_{H_2SO_4}$ = 2.22 X 10^{-5}cm^2/sec[15].

Fig. 7, was constructed to measure bubble sizes. Two of the walls are 1 cm X 5 cm X 10 cm optical glass flats. These are separated by two strips of 1/8 inch rubber gasket material which form the remaining two walls. The same cathodes used on the cell for measuring hydrogen concentrations were bolted to the bottom of this cell to form the electrolyte compartment. One and two molar sulphuric acid electrolytes were used, and a strip of platinum sheet inserted into the top of the cell was used as an anode.

Photomicrographs of the bubbles were taken through the glass walls of the cell and are shown in Fig. 8. Pictures taken at the electrode surface, and at heights of five and ten centimeters above the surface showed no difference in bubble size indicating that essentially all the growth occurs while the bubble is still attached to the cathode. There was no difference in bubble size between the two cathodes. At current densities of 2.5 and 25 ma/cm^2, where correlations with the surface renewal model were tested, the average bubble diameters were identical at 4×10^{-3} cm. The bubble diameter increased to 8×10^{-3} cm at 250 ma/cm^2.

The average bubble diameter was obtained by measuring the sizes of all bubbles in a specified area of the photograph and plotting the sizes on probability paper. The results are shown in Fig. 9. The size distribution of bubbles is normal, as indicated by the straight line in the probability plot, with a standard deviation in bubble diameter of 1.1×10^{-3} cm.
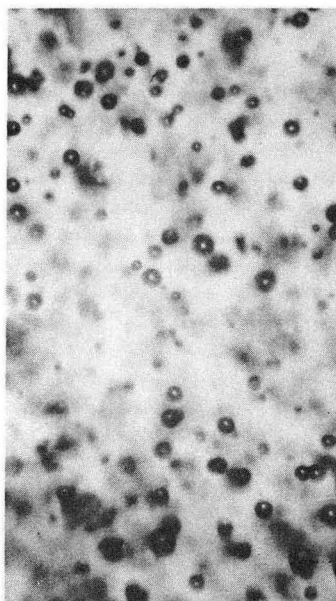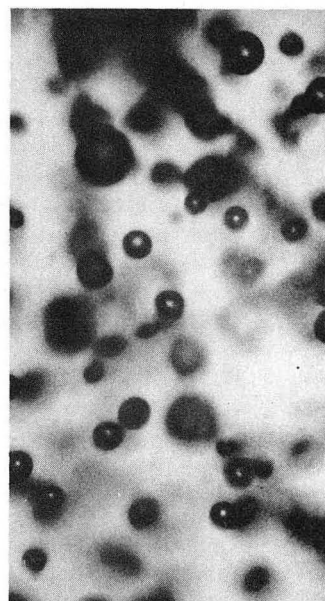
XBL 704-885

Fig. 7. Diagram of cell used for measuring hydrogen bubble size at cathode.
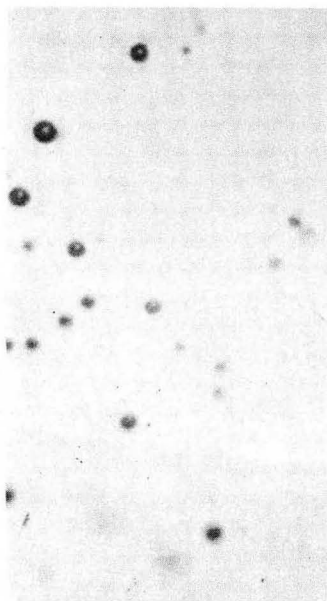
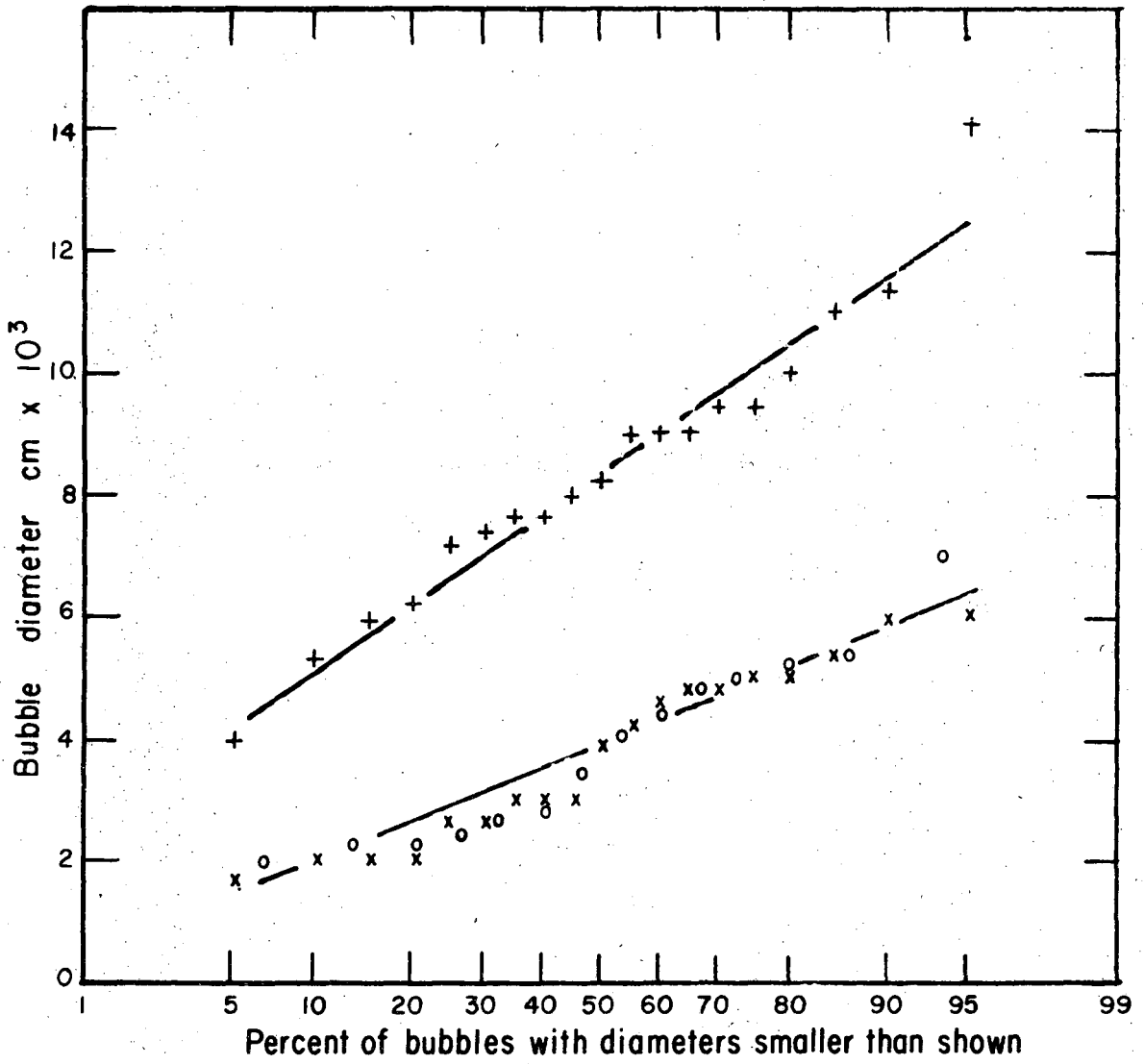2.5 ma/cm^2 25 ma/cm^2 250 ma/cm^2

XBB 678-4501

Fig. 8. Photographs of electrolytically generated H$_2$ gas
         1 mole/liter H$_2$SO$_4$ Smooth Pt cathode Magnification x40

-18-

Fig. 9. Probability plot of bubble size being discharged from smooth Pt cathode.

   o 2.5 ma/cm^2 x 25 ma/cm^2 x 250 ma/cm^2

XBL 704-883

RESULTS

Concentration Profiles

The hydrogen concentration in the electrolyte as a function of distance from the cathode extrapolated to the time of current interrruption is shown in Fig. 10. Concentration is expressed as pressure of hydrogen in equilibrium with the solution. Points at X = 0 were obtained from the potential decay curves at the cathode and are in line with the points obtained from the ring electrodes.

In the vicinity of the cathode, the hydrogen concentration curves are approximately logarithmic. By measuring the slopes in Fig. 10, concentration gradients can be calculated using Eq. (2).

$$\frac{dC}{dx} = P \frac{C_E}{P_o} 2.3 \frac{d \log P}{dx} \tag{2}$$

The experimental concentration gradient obtained from Fig. 10 and Eq. (2) can be used in the diffusion equation to calculate the hydrogen diffusion flux at any distance from the cathode

$$W = D \frac{dC}{dx} \tag{3}$$

The diffusion flux is highest at the cathode surface, and decreases further from the cathode as more of the gas is transported by convection and by bubbles. The hydrogen diffusion flux calculated at the electrode surface is compared in Table II with the total amount of gas being generated.
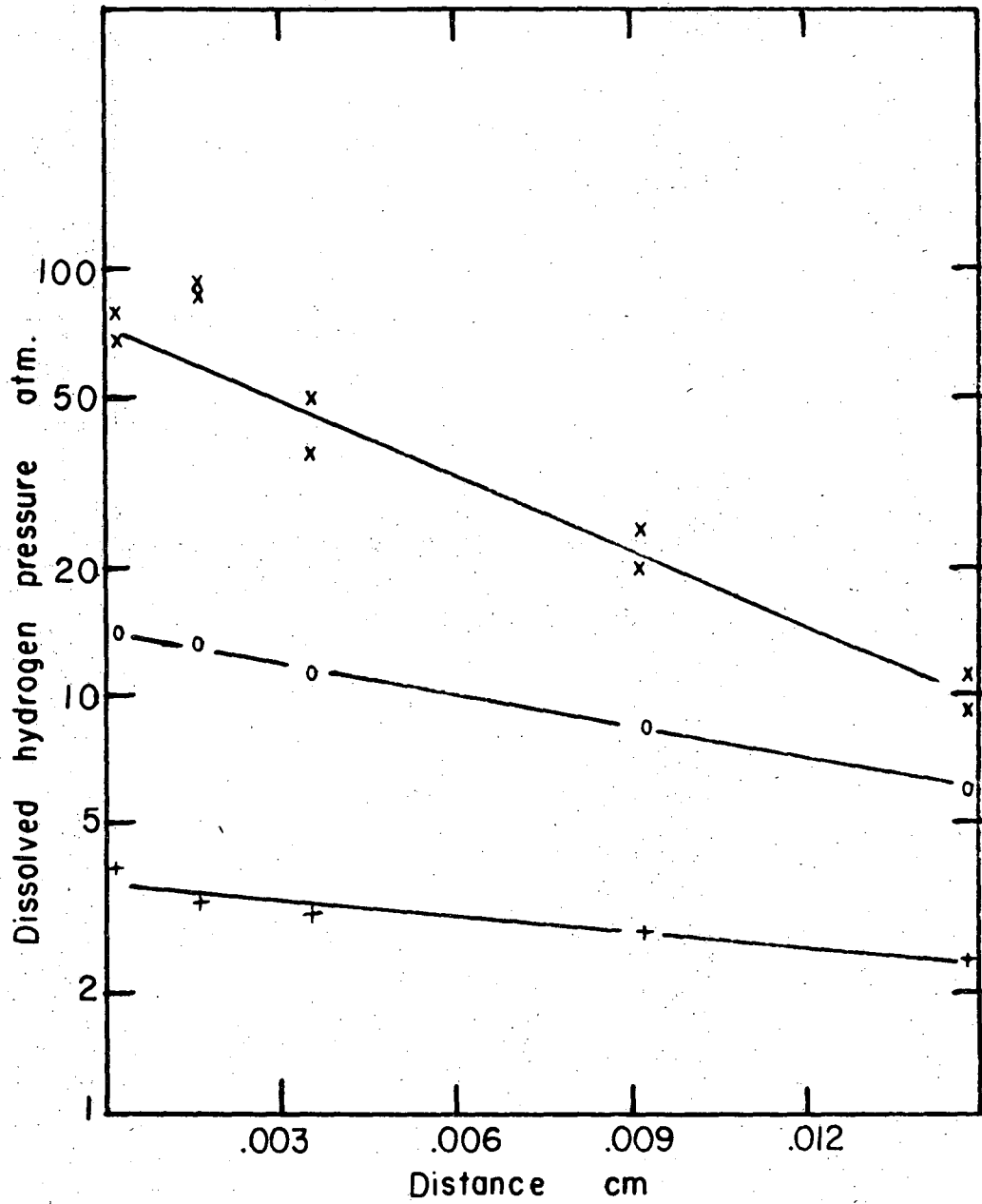
Fig. 10. Dissolved hydrogen concentration as a function of distance from polished platinum cathodes.

    x 39.5 ma/cm^2 o 3.95 ma/cm^2 x .395 ma/cm^2

XBL 704-887

Table II

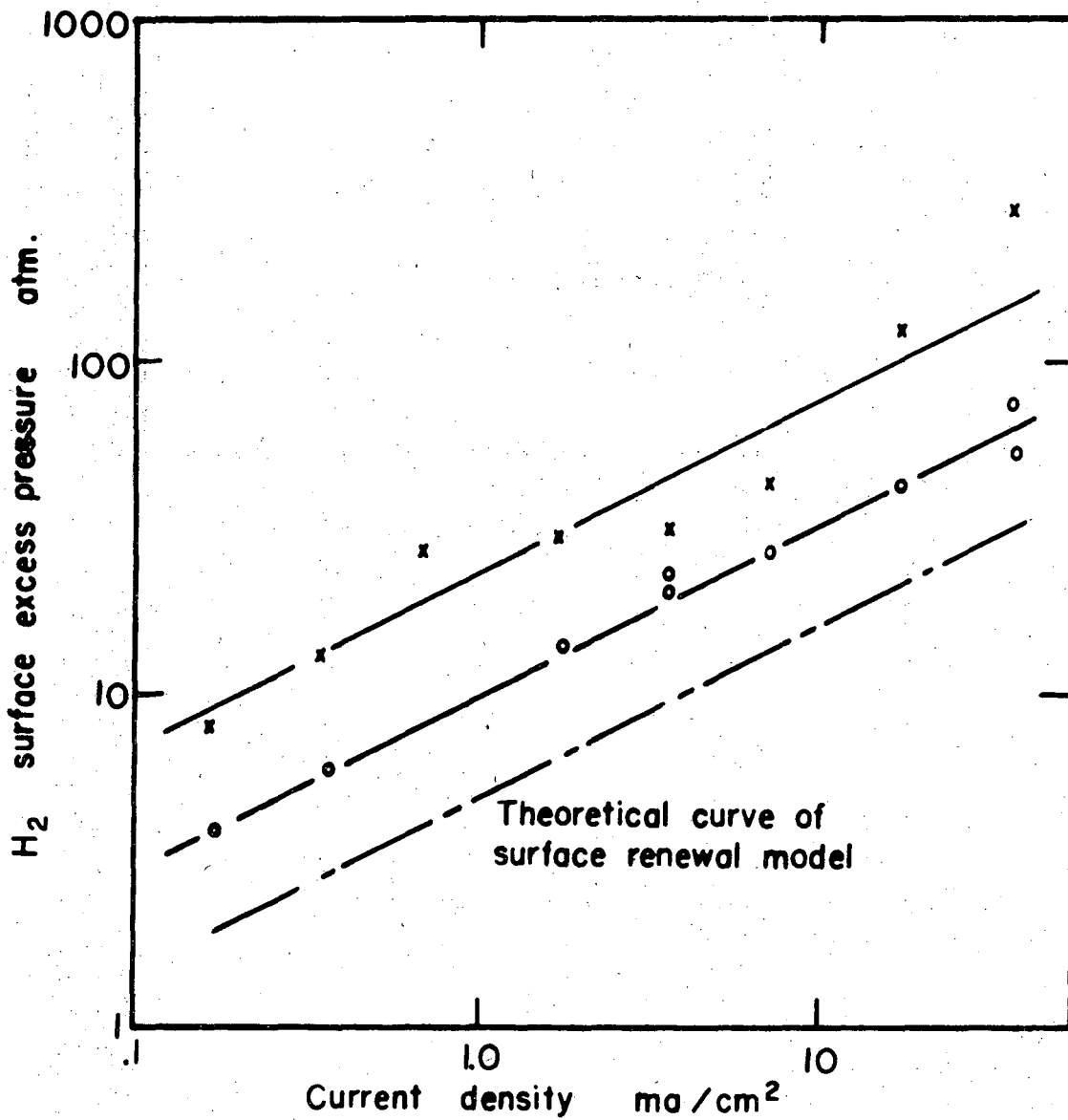| Current Density ma/cm^2	Hydrogen Generation Rate $moles/cm^2 sec$	Hydrogen Flux* (corrected for surface covered by bubbles) $moles/cm^2 sec$
.395	2.04×10^{-9}	2.40×10^{-9}
3.95	2.04×10^{-8}	2.20×10^{-8}
39.5	2.04×10^{-7}	2.46×10^{-7}

The discrepancy between the flux calculated from the current density and that obtained from the measured concentration gradient is a result of: (1) uncertainty in the shape of the concentration-distance curve (Theory does not predict the shape of the curve; the logrithmic function was chosen because it fits the data fairly well), and (2) lack of an exact value of the concentration at a given distance from the cathode (since concentration at any point varies in a cyclic manner depending on the stage of bubble growth in the immediate vicinity).

Supersaturation at the Cathode

The hydrogen supersaturation at platinized platinum and at smooth platinum cathodes was evaluated as a function of current density, and the results are plotted in Fig. 11. A surface-renewal model is tested to predict the concentration of dissolved hydrogen at the cathode surface as a function of the current density. Physically the model assumes that all hydrogen leaves the electrode by unsteady state diffusion.

*Calculated from concentration gradients at x = 0

Fig. 11. Hydrogen supersaturation in electrolyte at cathode surface as a
function of current density.

x   polished platinum cathode
o   platinized platinum cathode

The diffusion process starts when a bubble leaves the cathode surface, and the space occupied by the bubble is replaced by fresh electrolyte from the bulk of the solution. Transient diffusion now takes place into the fresh electrolyte until the concentration of gas at the cathode surface becomes great enough to cause a new bubble to nucleate. After this new bubble has grown large enough to be discharged, it too is replaced by fresh electrolyte and the process begins again.

The surface-renewal model is a great simplification of the events occurring around a cathode. It was first formulated by Higbie[16] to account for gas bubbles dissolving in liquids and has also been success-fully included in heat transfer models involving bubble generation at a heated surface by nucleate boiling (Han and Griffith,[17] Engelberg-Forster and Grief[18]). More recently, and more directly connected to electrochemistry, it was applied by Venezel[13] to interpret the observed rate of transfer of ferric ions to a cathode while hydrogen gas is being evolved.

To calculate hydrogen concentration with a surface-renewal model requires no empirical constants - only the physical properties of the system and the average time between discharge of bubbles from a location on the cathode. Optical measurements of the bubble size were made to calculate the time between bubbles. All bubbles were close to the same size with an average diamter of 4×10^{-3} cm, independent of the current density over the range used in this study. The rate of bubble genera-tion can be calculated by dividing the hydrogen production rate by the

average bubble volume and is given by[*]

$$N = \frac{3I}{4\pi r^3 nF\rho_V}$$ (4)

Assuming that the bubbles being generated have an equal chance of forming anywhere on the cathode, the average time between bubbles forming at a location is

$$t = \frac{1}{NA}$$ (5)

By assuming that the bubbles are spheres when discharged and that the effective area for surface-renewal is the area shielded by the bubbles, the time between bubbles is obtained by combining Eqs. (4) and (5).

$$t = \frac{4\,\rho_V nFr}{3I}$$ (6)

The average hydrogen concentration at the electrode can now be obtained by integrating equation 1 for concentration over the time interval between bubbles given in Eq. (6), dividing by the average time, and evaluating the concentration at $X = 0$, the electrode surface. Expressed in dimensionless form, the excess hydrogen pressure at the cathode surface is given by Eq. (7).

---

[*] This assumes that essentially all the growth occurs in the immediate vicinity of the cathode, which is substantiated by our observation that no difference could be measured between the size of bubbles being evolved from the electrode and bubbles several centimeters above the surface.

$$p_S/P_0 = \frac{P_S - P_B}{P_0} = .665 \quad \frac{\rho_V r I}{C_0^2 DF(1-\theta)} \tag{7}$$

An increase in the effective current density on the cathode due to surface coverage by bubbles is accounted for by the $(1-\theta)$ term of Eq. (7), where θ represents the fraction of the electrode area shielded by bubbles. Using the measured hydrogen concentration from Fig. 10, the time for a bubble to grow from nucleation to the size of discharge can be calculated by the method of Cheh.[11] The average surface covered by bubbles is obtained by taking the ratio of the time an area is covered during the growth of a bubble to the time between bubbles. Calculated values for surface coverage are 1%, 2%, and 4% at current densities of 0.4, 4, and 40 ma/cm^2. Thus the correction for the electrode area covered by bubbles in these experiments is small, and of the same order of magnitude as the values reported by Venezel,[13] based on optical observation.

According to the model, at low surface coverage the hydrogen surface excess is proportional to the square root of the current density. The 1/2 slopes of the lines in Fig. 11 placed by visual inspection,[*] appear to yield a good fit of experimental data for platinized platinum; less so for smooth platinum cathodes. Both lines, however, are substantially above the one representing surface renewal model.

---

[*] A multiple regression correlation of the data in Fig. 11 gives for the platinized platinum case
$$P_s = 3.11 \ I^{.51}$$
The limits on the exponent of I (at the 95% confidence level) are .45 to .53. For the smooth platinum electrode the equation is
$$P_s = 5.75 \ I^{.59}$$
with limits on the exponent of .41 to .76 at the 95% confidence level.

One of the basic assumptions of the surface-renewal model is that bubbles have an equal likelihood of forming at any point on the cathode. If this is not the case and certain areas are less active for nucleating bubbles, more gas must diffuse from these areas, and the average length of the diffusion path is longer. The average gas concentration at the cathode would increase, and the curves plotted in Fig. 11 would be displaced upward as is observed particularly with the unplatinized electrode. Thus the increased concentration at the unplatinized cathode is likely to be the result of difficulty in nucleating bubbles.

Since higher nucleation energy increases the supersaturation, it might appear that eliminating the nucleation energy would eliminate supersaturation. This, however, is not the case. Although bubbles could form at low values of supersaturation, very small concentration gradients would exist to further their growth. With the logrithmic concentration profile plotted in Fig. 10, if the nucleation energy were low enough so that a bubble could form whenever the supersaturation reached three atmospheres, a calculation by the method presented by Cheh[11] shows that the bubble would require two seconds to grow large enough to leave the cathode. At 40 ma/cm^2 a bubble must be discharged from each location on the cathode every 3 seconds, and the θ term in Eq. (7) representing fraction of the electrode covered with bubbles would approach 1. In the extreme case the electrode would become completely covered with gas, a phenomenon ("anode effect") indeed observed in the electrolysis of molten salts.

When the results of Breiter, Kammermaier and Knorr,[7] who measured surface concentration with an AC phase-shifting technique on an activated

platinum cathode, are plotted as surface concentration vs current density,
the curve shown in Fig. 12 is obtained. Our data on the platinized
platinum electrode are shown for comparison. In the experiments of
Breiter, et al., mechanical agitation was supplied in addition to the
free convection caused by gas evolution.

In Fig. 13 the mass-transfer coefficient for the transport of
hydrogen gas from the electrode

$$K = \frac{I}{nF(C_S - C_B)} \qquad (\varepsilon)$$

is plotted vs. current density.

Below 20 ma/cm^2 the coefficient of mass transfer from the data of
Breiter, et al., is constant, indicating that the mass transfer rate is
controlled by mechanical agitation, and is not affected by the rate of
gas evolution. At higher current densities the gas evolved at the
cathode provides more effective agitation than the mechanical stirring,
and the mass-transfer coefficient increases. In the results reported
here no mechanical agitation is provided, and the mass-transfer coef-
ficient is approximately proportional to the square root of the current
density over the entire range studied. It is worth noting that above
100 mA/cm^2 the two mass transfer coefficients calculated from experimental
data of Breiter, et al., fall close to the best line of slope = 1/2
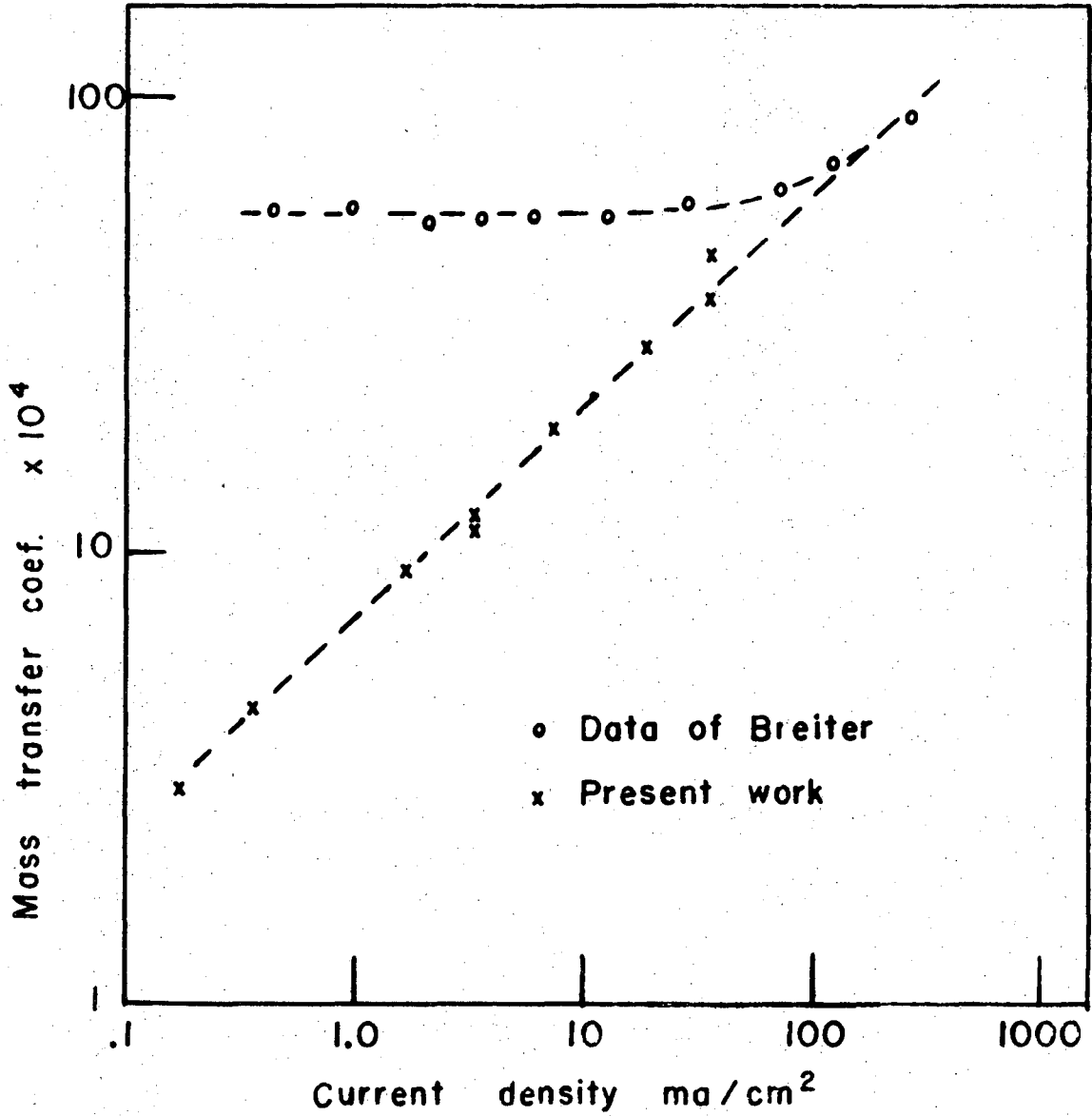representing the mass-transfer coefficients obtained in the present work.
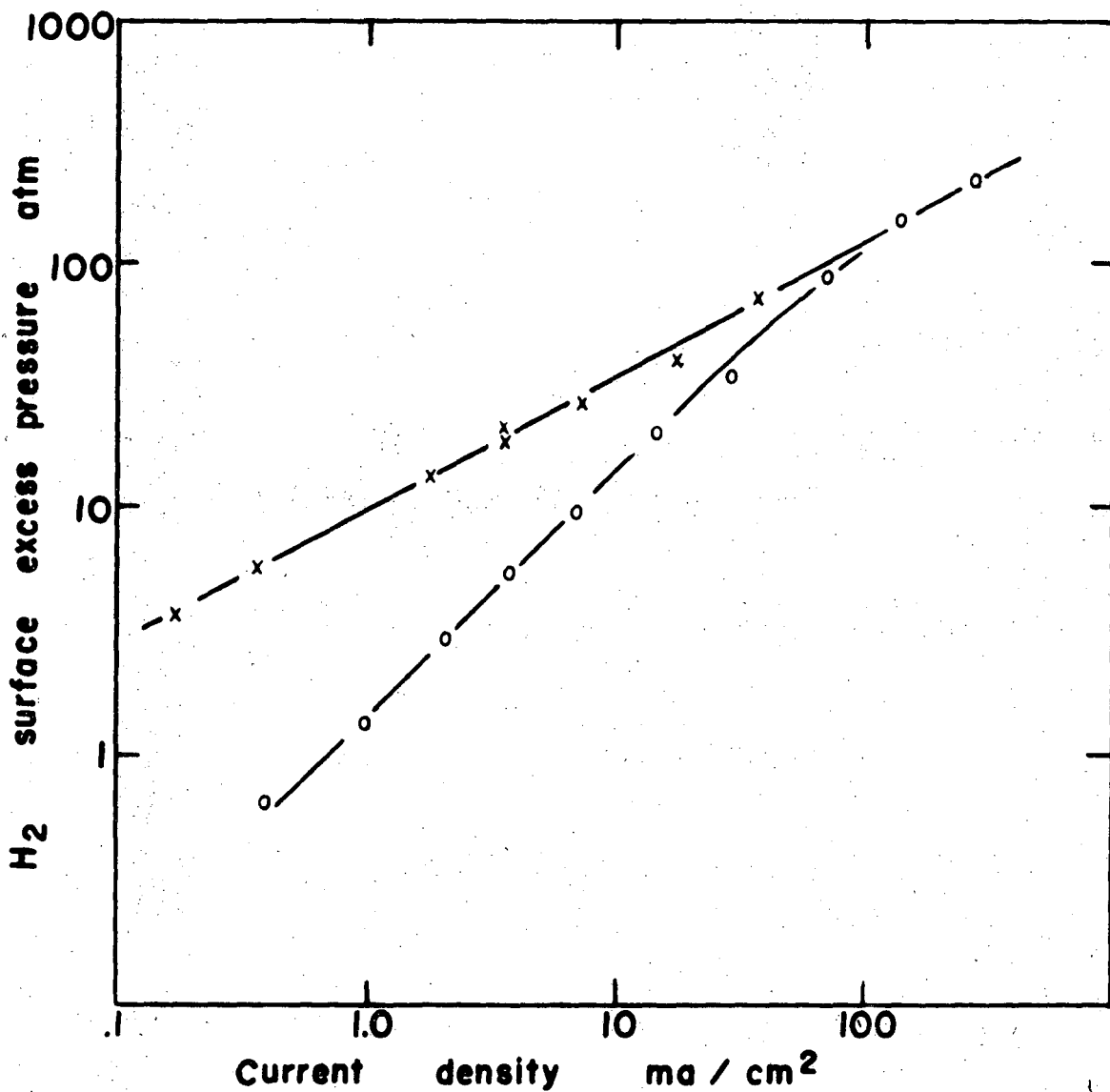
XBL 704-879

Fig. 12. Hydrogen supersaturation at cathode surface as a function of
current density.

        o   Data of Breiter, Kammermaier and Knorr[7]
        x   Present work

Fig. 13. Mass transfer coefficient for dissolved hydrogen gas leaving cathode as a function of current density.

XBL 704-888

CONCLUSIONS

It has been demonstrated that substantial levels of gas supersaturation exist at a horizontal cathode at which hydrogen is discharged without mechanical agitation. The major portion of the hydrogen leaves the cathode surface by diffusing through the solution to a nearby bubble on the cathode surface. Supersaturation provides the driving force for diffusion. The generation of bubbles very effectively agitates the electrolyte adjacent to the cathode surface, bringing in electrolyte from the bulk of the solution. The mass transfer coefficient for dissolved gas is approximately proportional to the square root of the current density; the same relationship has been proposed for the mass transfer coefficient of ionic transport at gas evolving electrodes (Ibl[19]). The proposed surface renewal model predicts the square root dependence of supersaturation on current density, but the levels of supersaturation calculated by this simple method are lower than those obtained from potential measurements.

This discrepancy is much greater in the case of smooth platinum surfaces where large energies are required for bubble nucleation, than in the case of rough, or porous surfaces, such as on platinized platinum.

ACKNOWLEDGMENTS

NOMENCLATURE

Symbols

A	Surface area covered by a bubble	cm^2
C	Concentration	$moles/cm^3$
D	Diffusion coefficient	cm^2/sec
F	Faraday constant	coulomb/mole
I	Current density	$amperes/cm^2$
K	Mass transfer coefficient	cm/sec
N	Bubble generation rate	$bubbles/cm^2 sec$
n	Electrons transferred	
P	Pressure	atmospheres
p	Excess pressure over bulk electrolyte	atmospheres
r	Bubble radius	cm
t	Time	seconds
W	Mass flux	$moles/cm^2 sec$
x	Distance	cm
θ	Fraction of electrode area covered by bubbles	
ρ	Density	$moles/cm^3$

Subscripts

B	Bulk electrolyte
E	Equilibrium at atmospheric pressure
O	Atmospheric pressure
S	Surface of electrode
V	Vapor

BIBLIOGRAPHY

1. H. S. Carslaw and J. C. Jaeger, "Conduction of Heat in Solids," p. 63, Oxford (1959).

2. V. Levich, "Physicochemical Hydrodynamics," Prentis Hall, Englewood Cliffs, N. J., (1962).

3. "International Critical Tables," Vol. III, p. 272.

4. E. A. Aikazyan and A. I. Federova, Dolk. Akad. Nauk. SSR, 86, 1137 (1952).

5. B. Kabanov and A. Frumkin, Z. Physic. Chem. (Leipzig) 165A, 433-52 (1933).

6. M. Breiter, "Transactions of Symposium on Electrode Process," E. Yeager, ed., John Wiley, (1961) pp. 307-24.

7. M. Breiter, H. Kammermaier and C. A. Knorr, Z. Electrochem. 60, 37, 119, 455, (1956).

8. M. Becker and M. Breiter, Z. Electrochem. 60, 1081 (1956).

9. J. A. S. Green and F. A. Lewis, Trans. Faraday Soc. 60, 2234-43 (1964).

10. J. P. Glas and J. W. Westwater, Int. J. Heat and Mass Transfer 7, 1427-43 (1964).

11. H. Y. Cheh, Dissertation, University of California, Berkeley (1967).

12. Ives and Janz, Reference Electrodes, AP, 107 (1961).

13. J. Venezel, Dissertation, ETH, Zurich, No. 3019 (1961).

14. R. Parsons, Handbook of Electrochemical Constants, 87, Butterworth (1939).

15. James, Hollingshead and Gordon, J. Chem. Phys. 7, 89 (1939).

16. R. Higbie, Trans. Am. Inst. Chem. Engrs. 31, 365-89 (1935).

17. C. V. Han and P. Griffith, Intern. J. Heat Mass Transfer 8, 905 (1965).

18. Engleberg-Forster and Grief, Trans ASME J. Heat Transfer 81, 43 (1959).

19. N. Ibl, Chemic-Ingenieur-Technik 35, 353 (1963).